Available online at www.sciencedirect.com
ScienceDirect
Journal of Magnetic Resonance 183 (2006) 203–212
JMR Journal of Magnetic Resonance
www.elsevier.com/locate/jmr

Effects of radiation damping on *Z*-spectra

David C. Williamson [a], Johanna Närväinen [b], Penny L. Hubbard [b], Risto A. Kauppinen [c], Gareth A. Morris [b,*]

[a] *Department of Chemistry, University of York, Heslington, York YO10 5DD, UK*
[b] *School of Chemistry, University of Manchester, Oxford Road, Manchester M13 9PL, UK*
[c] *School of Sport and Exercise Sciences, University of Birmingham, Birmingham B15 2TT, UK*

Received 8 June 2006; revised 11 August 2006
Available online 18 September 2006

Abstract

Radiation damping induced by the strong water magnetization in *Z*-spectroscopy experiments can be sufficient to perturb significantly the resultant *Z*-spectrum. With a probe tuned to exact electrical resonance the effects are relatively straightforward, narrowing the central feature of the *Z*-spectrum. Where, as is commonly the case, the probe is tuned sufficiently well to give optimum signal-to-noise ratio and radiofrequency field strength but is not at exact resonance, radiation damping introduces an unexpected asymmetry into the *Z*-spectrum. This has the potential to complicate the use of *Z*-spectrum asymmetry to study chemical exchange, for example in the estimation of pH *in vivo*.

Keywords: Radiation damping; *Z*-spectroscopy; Probe tuning; Magnetization transfer; Chemical exchange

1. Introduction

Radiation damping (RD) occurs because rotating transverse nuclear magnetization induces a current in the receiver coil, generating a rotating magnetic field and thus producing a torque on the magnetization. In high magnetic fields, RD is known to disturb NMR experiments such as relaxation measurements [1,2] and two-dimensional spectroscopy [3]. It is shown here that RD can also give rise to unexpected effects in *Z*-spectroscopy [4], the detection of magnetization exchange between water and macromolecules by measurement of the water magnetization as a function of the frequency of low-power RF pre-irradiation. Strong nuclear magnetizations can also perturb their own evolution through the dipolar demagnetizing field [5], but as the interactions involved are typically of the order of Q (the probe quality factor) times smaller than in radiation damping, they are neglected in what follows.

The phenomenon of radiation damping has been known for almost as long as nuclear magnetic resonance has been studied. As far back as 1949, Suryan [6] first proposed the interaction of an RF coil with the bulk magnetization of a sample as an explanation for the discrepancy between theoretical predictions of relaxation times and experimental observation. Bloembergen and Pound [7] formulated Suryan's hypothesis mathematically by combining the Bloch and Maxwell equations, coining the phrase "radiation damping". Bruce et al. [8] highlighted an erroneous assumption in the original Bloembergen paper, but the steady-state limit is the same in both descriptions. Building on the previous work, Bloom [9] published modified Bloch equations in which the effects of RD are included directly in a set of non-linear differential equations describing the motion of bulk magnetization. Bloom successfully described the effects of RD on the lineshapes of continuous wave (CW) experiments with and without relaxation, and highlighted the effects on adiabatic rapid passage. Szöke and Meiboom [10] showed that for flip angles between 90° and 270° the free induction decay following a single pulse passes through a maximum before decaying, drawing

* Corresponding author. Fax: +44 161 275 4598.
E-mail address: g.a.morris@manchester.ac.uk (G.A. Morris).

1090-7807/$ - see front matter © 2006 Elsevier Inc. All rights reserved.
doi:10.1016/j.jmr.2006.08.011

attention to the fact that the term ''radiation damping'' is something of a misnomer.

Although RD is an intrinsic physical phenomenon in all NMR experiments, the magnitude of the damping field depends on the Q value, the filling factor of the probe, and on the bulk magnetic moment of the sample, which in turn depends on the static field strength. As a result, RD is normally only observed in proton or fluorine experiments, and even then only with high concentrations at high fields. In order to make their observations at 0.704 T, Szöke and Meiboom artificially increased the Q of their receiver coil using positive feedback or ''Q-multiplication'' [10]. After this initial flurry of interest, little work was published on RD, mostly due to the fact that at the static field strengths then available the effects are generally negligible.

As technology has advanced and both static field strengths and probe Q values have increased, a renewed interest in RD has developed. In 1989 Warren et al. [11] described the effects of RD during soft pulse irradiation, and since then articles have appeared describing RD effects on multiplet shape [12], solvent suppression [13], T_1 [2] and T_2 [1] measurements, the use of RD to determine chemical exchange rates [14,15], and radiation damping-induced spurious peaks in 2D spectroscopy [16,17]. RD has been shown to influence *in vivo* MRI experiments; in the determination of cerebral blood flow, RD effects in T_1 experiments can be greatly reduced by applying a small field gradient during the inversion time [18]. RD has also been observed in hyperpolarized ^{3}He at 1.5 T, used in imaging of lungs [19]. A good deal of work has been carried out describing inhomogeneous line broadening in the presence of RD using an isochromat model [1,20–23], provoking an interesting and significant response [24] regarding the appropriateness of the model in this case. RD has been reviewed recently by Augustine [25], and Mao and Ye [26].

One topic that has received rather less attention is the effect of RD when a probe is not at exact electrical resonance [12,17,27]. Traditionally, severe detuning of the probe has been used as a method of reducing the effects of RD, in a trade-off against signal-to-noise ratio. Detuning reduces the line broadening effects of RD both by reducing the induced current, and by reducing the angle between the precessing magnetization and the secondary radiofrequency field generated by the coil. Even slight detuning has been shown to introduce unexpected effects in multiplet patterns [12]. This is significant because the conventional method of probe tuning, by minimizing reflected power, is relatively inaccurate [27]. Two significant factors here are the practical difficulty of ensuring a purely resistive source impedance, and the fact that reflected power varies only quadratically with electrical resonance offset for small offsets. The frequency of minimum reflectance may be some hundreds of kHz from exact electrical resonance; it is shown here that this can significantly distort Z-spectra, and can have dramatic effects on saturation dynamics.

Although the idea of using NMR to measure magnetization transfer (MT) between spin pools was common [28] well before the 1990s, Grad and co-workers [4,29] were the first to use the term Z-spectroscopy to describe the measurement of the perturbation of a solvent's Z-magnetization as a function of the frequency of a long off-resonance saturation pulse. The pre-saturation pulse affects the solvent via the exchange of magnetization, through a variety of possible mechanisms, between the solvent and another magnetization pool or pools. In their work, Grad and co-workers explored MT between the liquid-like and solid-like components of a heterogeneous mixture as a route to determining the NMR properties of the largely NMR-invisible solid-like component. The early 1990s saw a sudden increase in the study of MT, largely due to the work of Wolff and Balaban [30], who demonstrated that the contrast in an MR image could be changed using off-resonance saturation pulses. Since Grad and Bryant's studies, a great deal of work has been carried out using Z-spectra and a variety of theoretical approaches have been developed to extract meaningful physical parameters from the data [31–39]. In general, the early work assumed that dipole–dipole cross relaxation was the dominant mechanism for MT, but more recently there has been increased interest in studying chemical exchange pathways, driven in part by the search for a pH-dependent MR contrast mechanism [40–42]. Many of these studies exploit the observation that the MT between water protons and the protons of mobile protein sidechains, a process dominated by chemical exchange, produces an asymmetry in the Z-spectrum and that this asymmetry can be used to determine pH.

In this work, the effects of RD and probe tuning on the shape and asymmetry of Z-spectra are examined both theoretically and experimentally, in a one-pool system and in an exchanging two-pool model. It is shown that under commonly encountered conditions, the combination of RD and inexact tuning can lead to a relatively large asymmetry in the steady-state Z-spectrum, potentially complicating the interpretation of (pH-dependent) exchange-induced asymmetry. It is also demonstrated that in experiments using short irradiation times, comparable to the T_2 of the water pool, RD can change the shape of the Z-spectrum very significantly.

2. Theory

2.1. One-pool model

The Bloch equations [43] for a single spin pool, modified to include the effects of radiation damping and of the electrical detuning of the probe [12], become

$$\begin{aligned}\frac{dM_x}{dt} &= -\beta M_x - \delta M_y - k_d M_x M_z \cos^2\theta - k_d M_y M_z \cos\theta \sin\theta \\ \frac{dM_y}{dt} &= -\beta M_y + \delta M_x - \omega_1 M_z - k_d M_y M_z \cos^2\theta + k_d M_x M_z \cos\theta \sin\theta \\ \frac{dM_z}{dt} &= -\alpha(M_z - M_0) + \omega_1 M_y + k_d (M_x^2 + M_y^2)\cos^2\theta \end{aligned} \tag{1}$$

where $\alpha = 1/T_1$, $\beta = 1/T_2$, δ is the offset from (magnetic) resonance in rad s^{-1}, ω_1 is the RF amplitude in rad s^{-1}, and k_d is the proportionality constant between the damping field (again in frequency units) and transverse magnetization. For a coil of quality factor Q and filling factor f, $k_d = Qf\gamma\mu_0/2$ where γ is the magnetogyric ratio and $\mu_0 = 4\pi \times 10^{-7}$ NA^{-2} is the permeability of free space. If the coil is tuned to a centre frequency ω_0 and the radiofrequency is ω, then in terms of the dimensionless electrical resonance offset parameter $\Delta = (\omega - \omega_0)/\omega_0$ the detuning angle θ is given by

$$\theta = \arctan\left[\frac{Q\Delta(2+\Delta)}{(1+\Delta)}\right]. \tag{2}$$

The Z-spectrum may be found by setting the time derivatives of Eq. (1) to zero and solving the resultant cubic equation Eq. (3) for $M_z(\infty)$ either analytically using the Cardano method [44] or numerically using the Laguerre method [45]

$$\begin{aligned} &k_d^2 \alpha \cos^2\theta M_z(\infty)^3 + k_d \alpha \cos\theta (2\delta \sin\theta + 2\beta\cos\theta \\ &\quad - k_d M_0 \cos\theta) M_z(\infty)^2 + [\alpha(\delta^2+\beta^2) + \omega_1^2 \beta \\ &\quad - 2k_d \alpha M_0 \cos\theta(\beta\cos\theta + \delta\sin\theta)] M_z(\infty) \\ &\quad = \alpha(\delta^2+\beta^2) M_0. \end{aligned} \tag{3}$$

For small θ and $k_d M_0 \ll \omega_1$, series expansion of the analytical expression for the asymmetry of the Z-spectrum ($M_z(\delta) - M_z(-\delta)$) to the 1st order in θ and k_d yields extrema at $\delta = \pm\omega_1\sqrt{\beta/\alpha}$, of magnitude $\pm(k_d M_0^2/2\omega_1)\sqrt{\alpha/\beta}$.

The x and y components can be obtained by substituting the solution of Eq. (3) into Eqs. (4) and (5)

$$\begin{aligned} M_x(\infty) &= \frac{(\delta + M_z(\infty) k_d \cos\theta \sin\theta)\omega_1 M_z(\infty)}{(\delta + M_z(\infty) k_d \cos\theta\sin\theta)^2 + (\beta + k_d M_z(\infty)\cos^2\theta)^2}, \\ M_y(\infty) &= -\frac{(\beta + k_d M_z(\infty)\cos^2\theta)\omega_1 M_z(\infty)}{(\delta + M_z(\infty) k_d \cos\theta\sin\theta)^2 + (\beta + k_d M_z(\infty)\cos^2\theta)^2}. \end{aligned} \tag{4}$$

When the electrical circuit is correctly tuned, i.e., at electrical resonance $\theta = 0$, these results reduce to those reported by Bloom [9].

It is also helpful to consider the time-dependent solution to Eq. (1), to calculate the form of the free induction decay from a single pulse under the small flip-angle approximation $M_z \approx M_0$. The Bloch equations in M_x and M_y are no longer non-linear and their solution may be written as

$$\begin{aligned} M_{xy}(t) = &\exp[-(\beta + k_d M_0 \cos^2\theta)t] \exp[-i(\delta + k_d M_0 \\ &\times \sin\theta\cos\theta)t] \end{aligned} \tag{5}$$

in which M_x and M_y have been combined as $M_{xy} = M_x + iM_y$. In effect, the solution is identical in form to the solution of the standard Bloch equations under the same approximation, but with an additional line broadening and a frequency shift term due to the RD. The real part of the Fourier transform of Eq. (5) is a Lorentzian of width $\lambda = (\beta + k_d M_0 \cos^2\theta)/\pi$ Hz, with a frequency shift of $k_d M_0 \cos\theta\sin\theta$ Hz relative to an equivalent, undamped signal. If the linewidth in the absence of RD can be neglected, the RD constant k_d is approximately $\pi\lambda_{max}/M_0$, where λ_{max} is the width of the Lorentzian when the probe is on electrical resonance.

2.2. Two-pool model

In investigating the effect of RD on Z-spectroscopy a useful approximation is to consider a system of two spin pools with $M_0^a \gg M_0^b$ and $|\delta_a - \delta_b| \gg k_d$. In this approximation only pool **a** generates a significant RD field, and the field generated is too far off resonance to affect pool **b** directly. Unfortunately even with these simplifications the coupled equations are resistant to analytical solution. One drastic approximation, common in the literature [31–35], is to neglect the exchange of transverse magnetization, but this overestimates the coherence lifetimes of the two pools, giving rise to simulated Z-spectra in which the pool **b** feature is too narrow. An intermediate approximation that avoids this problem is to include the exchange terms in loss of transverse magnetization, but not those involving gain. Such a system is relatively tractable mathematically, and retains the basic features needed for successful modelling of experimental data under typical conditions. The Bloch equations for such a system become

$$\begin{aligned} \frac{dM_x^a}{dt} &= -\beta_a M_x^a - \delta_a M_y^a - k_d M_x^a M_z^a \cos^2\theta \\ &\quad - k_d M_y^a M_z^a \cos\theta\sin\theta - R_a M_x^a \\ \frac{dM_y^a}{dt} &= -\beta_a M_y^a + \delta_a M_x^a - \omega_1 M_z^a - k_d M_y^a M_z^a \cos^2\theta \\ &\quad + k_d M_x^a M_z^a \cos\theta\sin\theta - R_a M_y^a \\ \frac{dM_z^a}{dt} &= -\alpha_a\left(M_z^a - M_0^a\right) + \omega_1 M_y^a + k_d\left(M_x^{a^2} + M_y^{a^2}\right)\cos^2\theta \\ &\quad - R_a\left(M_z^a - M_0^a\right) + R_b\left(M_z^b - M_0^b\right) \\ \frac{dM_x^b}{dt} &= -\beta_b M_x^b - \delta_b M_y^b - R_b M_x^b \\ \frac{dM_y^b}{dt} &= -\beta_b M_y^b + \delta_b M_x^b - \omega_1 M_z^b - R_b M_y^b \\ \frac{dM_z^b}{dt} &= -\alpha_b\left(M_z^b - M_0^b\right) + \omega_1 M_y^b - R_b\left(M_z^b - M_0^b\right) \\ &\quad + R_a\left(M_z^a - M_0^a\right), \end{aligned} \tag{6}$$

where the parameters have the same meaning as in Eq. (1), and R_a and $R_b (= R_a M_0^a/M_0^b)$ are the rate constants for transfer of Z-magnetization from pool **a** to pool **b** and vice

versa, respectively. (Including the redundant M_0^a and M_0^b elements in the terms for exchange of Z-magnetization simplifies the subsequent elimination slightly.)

The transverse exchange terms may be lumped in with relaxation to give

$$\begin{aligned}
\frac{dM_x^a}{dt} &= -\beta'_a M_x^a - \delta_a M_y^a - k_d M_x^a M_z^a \cos^2\theta - k_d M_y^a M_z^a \cos\theta \sin\theta \\
\frac{dM_y^a}{dt} &= -\beta'_a M_y^a + \delta_a M_x^a - \omega_1 M_z^a - k_d M_y^a M_z^a \cos^2\theta \\
&\quad + k_d M_x^a M_z^a \cos\theta \sin\theta \\
\frac{dM_z^a}{dt} &= -\alpha_a\left(M_z^a - M_0^a\right) + \omega_1 M_y^a + k_d\left(M_x^{a^2} + M_y^{a^2}\right)\cos^2\theta \\
&\quad - R_a\left(M_z^a - M_0^a\right) + R_b\left(M_z^b - M_0^b\right) \\
\frac{dM_x^b}{dt} &= -\beta'_b M_x^b - \delta_b M_y^b \\
\frac{dM_y^b}{dt} &= -\beta'_b M_y^b + \delta_b M_x^b - \omega_1 M_z^b \\
\frac{dM_z^b}{dt} &= -\alpha_b(M_z^b - M_0^b) + \omega_1 M_y^b - R_b(M_z^b - M_0^b) + R_a(M_z^a - M_0^a),
\end{aligned} \tag{7}$$

where $\beta'_a = R_a + 1/T_2^a$ and $\beta'_b = R_b + 1/T_2^b$.

The steady-state solution for these equations is obtained in the same manner as for the one-pool model. The time derivatives are set to zero and the cubic Eq. (8) must be solved to obtain $M_z^a(\infty)$

$$\begin{aligned}
&Bk_d^2\cos^2\theta M_z^a(\infty)^3 + k_d\cos\theta(2B\delta_a\sin\theta \\
&\quad - \cos\theta\{A(k_d M_0^a\alpha_a - 2\beta'_a(\alpha_a + R_a)) \\
&\quad + (\delta_b^2 + \beta_b'^2)(k_d M_0^a(R_b\alpha_a + R_a\alpha_b) - 2R_b\alpha_a\beta'_a)\})M_z^a(\infty)^2 \\
&\quad + \left(B(\delta_a^2 + \beta_a'^2) + \omega_1^2\beta'_a\{A + R_b(\delta_b^2 + \beta_b'^2)\}\right. \\
&\quad - 2k_d M_0^a\cos\theta(\beta'_a\cos\theta + \delta_a\sin\theta) \\
&\quad \left.\{A\alpha_a + (R_b\alpha_a + R_a\alpha_b)(\delta_b^2 + \beta_b'^2)\}\right)M_z^a(\infty) \\
&\qquad = \left(\delta_a^2 + \beta_a'^2\right)\left(A\alpha_a + (R_b\alpha_a + R_a\alpha_b)(\delta_b^2 + \beta_b'^2)\right)M_0^a,
\end{aligned} \tag{8}$$

where

$$\begin{aligned}
A &= \alpha_b(\beta_b'^2 + \delta_b^2) + \omega_1^2\beta'_b \\
B &= A(\alpha_a + R_a) + R_b\alpha_a(\delta_b^2 + \beta_b'^2).
\end{aligned}$$

Once $M_z^a(\infty)$ has been determined, the other components of the magnetization vector may be found from

$$\begin{aligned}
M_x^a(\infty) &= \frac{\omega_1 M_z^a(\infty)\left(\delta_a + M_z^a(\infty)k_d\cos\theta\sin\theta\right)}{\left(\delta_a + k_d M_z^a(\infty)\cos\theta\sin\theta\right)^2 + \left(\beta'_a + k_d M_z^a(\infty)\cos^2\theta\right)^2} \\
M_y^a(\infty) &= \frac{-\omega_1 M_z^a(\infty)\left(\beta'_a + k_d M_z^a(\infty)\cos^2\theta\right)}{\left(\delta_a + k_d M_z^a(\infty)\cos\theta\sin\theta\right)^2 + \left(\beta'_a + k_d M_z^a(\infty)\cos^2\theta\right)^2} \\
M_x^b(\infty) &= \frac{R_a\delta_b\omega_1\left(R_b M_z^a(\infty) + \alpha_b M_0^a\right)}{AR_b} \\
M_y^b(\infty) &= \frac{-R_a\beta'_b\omega_1\left(R_b M_z^a(\infty) + \alpha_b M_0^a\right)}{AR_b} \\
M_z^b(\infty) &= \frac{R_a(\beta_b'^2 + \delta_b^2)(R_b M_z^a(\infty) + \alpha_b M_0^a)}{AR_b}.
\end{aligned} \tag{9}$$

3. Methods

3.1. NMR methods and samples

All data were acquired using a Varian INOVA 400 spectrometer. Z-spectra were measured by applying a low-power ($\omega_1/2\pi \approx 28$ Hz) saturation pulse for 20 s, followed by a small crusher gradient and ~10° flip-angle detection pulse to measure the steady-state Z-magnetization. A small flip-angle pulse was used in order to ensure approximately Lorentzian lineshapes irrespective of the strength of RD. A relaxation delay of 15 s was used between measurements. In experiments where the probe was detuned, the RF power levels for the saturation and detection pulses were adjusted to ensure constant ω_1. The Z-spectrum is a plot of the integrated peak area of the water signal versus the frequency of the saturation pulse. For Z-spectra of water, the saturation frequency was varied from −200 to 200 Hz (relative to the water line) in steps of 4 Hz and additional points were collected at ±300, ±400, ±500, ±700, ±1000, ±1500 and ±5000 Hz. For samples containing urea (two-pool model), measurements were made from −1000 to 1000 Hz in steps of 10 Hz, with additional points at ±1250, ±1500, ±2000, ±2500, ±3000, ±4000, ±5000 and ±10000 Hz.

Probe tuning was monitored by measuring reflected power as a function of frequency, following the manufacturer's instructions. Spin–lattice relaxation time was determined by inversion recovery with an additional field gradient between the 180° and 90° pulses to suppress RD effects. The radiofrequency field strength and small flip angle signal linewidth were determined using single pulse experiments.

The exchange rates and proton concentration ratio for the urea–water solution were determined via a Hoffmann–Forsén exchange experiment [28], in which pool **a** (water) was selectively inverted and the signals of pools **a** and **b** monitored during recovery. The peak integrals were fitted to the Bloch equations with exchange terms. The inversion delay was varied from 0 to 20 s in 63 steps, with a 20 s relaxation delay.

The one-pool system was studied using a 90% H_2O/10% D_2O mixture with a small quantity of acetone included as a reference. The model two-pool system was a 0.32 M solution of urea made up in pH 7 phosphate buffer solution containing 10% D_2O. All samples were measured in standard 5 mm NMR tubes, with the exception of one experiment, which used the same water mixture in a 2 mm outer diameter (1.6 mm i.d.) NMR capillary stem tube. All experiments were carried out at room temperature.

3.2. Data processing

The pulse width calibration, T_1 and T_2 calculations, and peak width and integral calculations were carried out using the manufacturer's standard software. All Z-spectroscopy data were Fourier transformed with 30 Hz line broadening. All fitting was carried out using the Levenberg–Marquardt

algorithm implemented in the Mathematica 5.1 software package (Wolfram Research Inc., Champaign, IL, USA). All parameters were fixed at experimentally determined values where possible; the position of exact magnetic resonance for pool **a** (f_0), the unsaturated water peak signal (S_0 proportional to M_0) and the RD constant ($k_d M_0$) were left as parameters to be fitted. The asymmetry $A(\Delta f) = S(f_0 + \Delta f) - S(f_0 - \Delta f)$ was calculated by taking a simple difference between the halves of the Z-spectrum $S(f)$. However, experimental determination of the exact water resonance frequency f_0 in the presence of RD is not straightforward and it is therefore difficult to ensure that experimental data points are spaced exactly equally either side of f_0. Experimental Z-spectra were therefore interpolated using a cubic spline when calculating the asymmetry $A(\Delta f)$.

4. Results and discussion

4.1. One-pool: simulations

Simulated Z-spectra for a single spin pool in a homogeneous magnetic field B_0, generated from the solution of Eq. (3), are shown in Fig. 1A. The RF field amplitude $\omega_1/2\pi$ was set to 40 Hz, and α and β were fixed at 0.33 and 0.50 s^{-1}, respectively. The spectra were generated with an RD strength $k_d M_0/\pi$ of 40 Hz and probe phase angles θ of 0 (on electrical resonance), 45° and −45°. These angles were chosen because the RD-related cross terms in the Bloch equations reach their maximum when the phase angle equals ±45°. While the roots of the derivative of the analytical solution to Eq. (3) are intractable, numerical simulations with realistic parameter values confirm that, as expected from the $\sin\theta\cos\theta$ cross terms in Eq. (1), the maximum asymmetry at all frequencies occurs at or close to $\theta = \pm 45°$. For reference, the Z-spectrum in the absence of RD is also shown. On electrical resonance, the effect of the RD is to narrow the Z-spectrum. The deviation from the undamped case is shown in the difference Z-spectra of Fig. 1B. The narrowing arises because the secondary field opposes the applied saturating field, reducing the effective RF amplitude. The maximum deviation is ca. 1% and since the Z-spectrum is symmetrical about zero frequency offset, the effects of RD are not visible in the asymmetry curves.

In contrast, when the probe is detuned, an asymmetry is introduced. The direction of this asymmetric twist depends on the direction of probe detuning. This RD-induced asymmetry may have consequences for the measurement of pH by Z-spectroscopy [41], where asymmetry plots are used to infer proton exchange rates and hence pH. The plots shown in Fig. 1C demonstrate that RD can cause Z-spectral asymmetry to arise even in the absence of

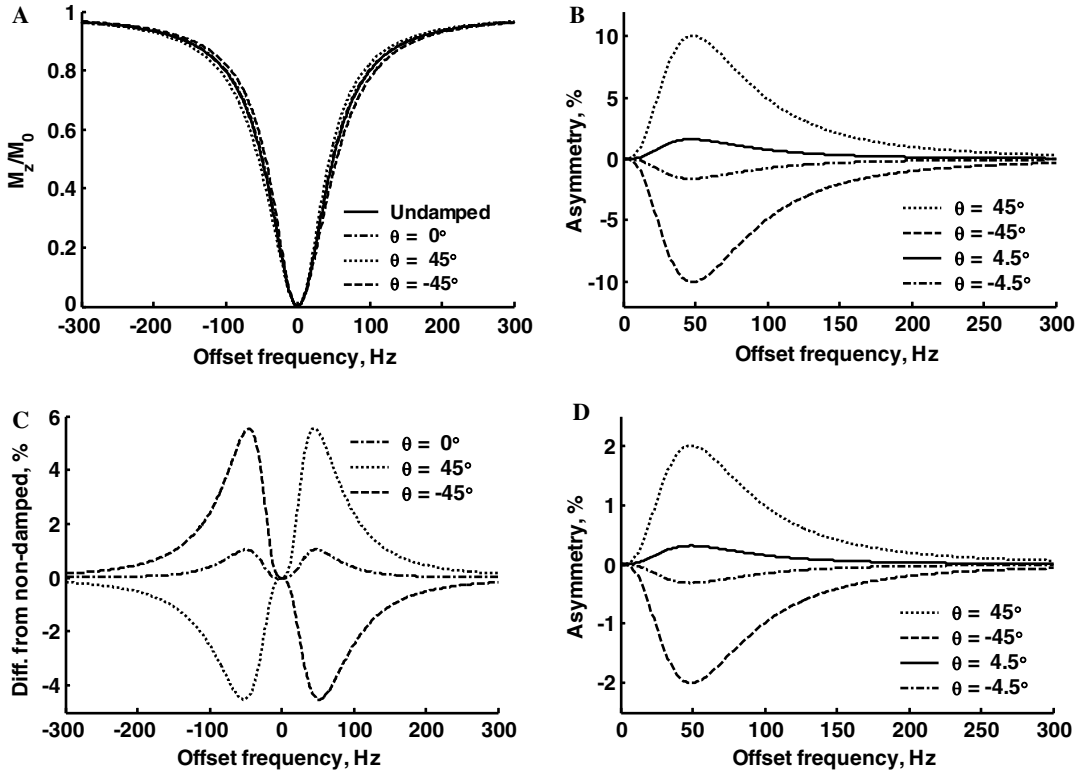

Fig. 1. (A) Simulated Z-spectra for a single spin pool at 400 MHz with a radiofrequency amplitude $\omega_1/2\pi$ of 40 Hz, a damping field $k_d M_0/\pi$ of 40 Hz, and α and β fixed at 0.33 and 0.50 s^{-1}, respectively. Data are shown for the undamped case (solid line) and in the presence of RD: on electrical resonance (probe phase angle $\theta = 0$, dash-dotted line) and for a detuned probe ($\theta = 45°$, dotted line, and $\theta = -45°$, dashed line). (B) Percentage difference between the undamped simulated Z-spectrum and damped simulations on (probe phase angle $\theta = 0$, dash-dotted line) and off ($\theta = 45°$, dotted line, and $\theta = -45°$, dashed line) electrical resonance. (C) Calculated Z-spectrum asymmetry with the above parameters for four different detuning angles. (D) as (C), but with a damping field $k_d M_0/\pi$ of 8 Hz.

exchange. The effect reaches a maximum here of 10% of the total Z-magnetization for a detuning angle of $\pm 45°$. Even for a much more modest tuning error, $\theta = \pm 4.5°$, the deviation is around 2%. For comparison, the asymmetry due to pH-dependent exchange *in vivo* typically amounts to no more than a few per cent. As RD is usually weaker *in vivo*, asymmetry curves for a reduced RD field of 8 Hz are presented in Fig. 1D.

It is easy to understand why the radiation damping affects only the flanks of the Z-spectrum. RD occurs only when significant transverse magnetization is present to induce a secondary radiofrequency field. Far from (magnetic) resonance the saturation pulse has only a small effect on the spins, and the bulk magnetization remains close to the z-direction until the detection pulse is applied. At steady state close to water resonance, the populations of the spin states are almost equal and leave little magnetization, transverse or longitudinal. In between these two extremes, the transverse magnetization rises to a maximum and RD has the greatest effect.

The asymmetry is related to the RD-induced shift in the water frequency during the FID, described by the term containing the factor $k_d \sin\theta\cos\theta$ in Eq. (5). During the saturation pulse, transverse magnetization generates RD and this causes the direct saturation effects to be different either side of the exact water resonance. For example, if the probe is tuned above electrical resonance, RD shifts the water resonance to higher frequency. When the system is irradiated at a negative offset frequency, the direct saturation is less than in a non-damped system. In contrast, at positive offset frequencies the water resonates closer to the irradiation frequency and this results in increased direct saturation. Detuning the probe below the electrical resonance causes the water resonance to shift to lower frequencies, and reverses the asymmetry.

For a given electrical detuning of the probe, the magnitude of the asymmetry depends on the ratio of the damping rate to the saturation RF amplitude. Fig. 2A shows the simulated asymmetry in a detuned probe ($\theta = -45°$) as the damping rate is varied, while keeping the RF amplitude constant at $\omega_1/2\pi = 200$ Hz. As expected, the effect of decreasing the damping field is to decrease, approximately linearly, the amplitude of the asymmetry in the Z-spectrum. If the RF amplitude is increased, the asymmetry feature becomes smaller in amplitude but broadens and moves further from resonance. This is shown in Fig. 2B for a detuning angle θ of $-45°$ and $k_d M_0/\pi$ of 50 Hz. All of these simulations assume, as noted above, a perfectly homogeneous B_0 field.

4.2. One-pool: experimental data

In order to estimate the probe Q, position of exact electrical resonance and strength of the damping field, small flip-angle spectra of the 90% H_2O/10% D_2O sample were acquired as a function of probe tuning, with the probe adjusted to give minimum reflected RF power at nine frequencies covering a range of 1.5 MHz (~0.4% of the proton Larmor frequency).

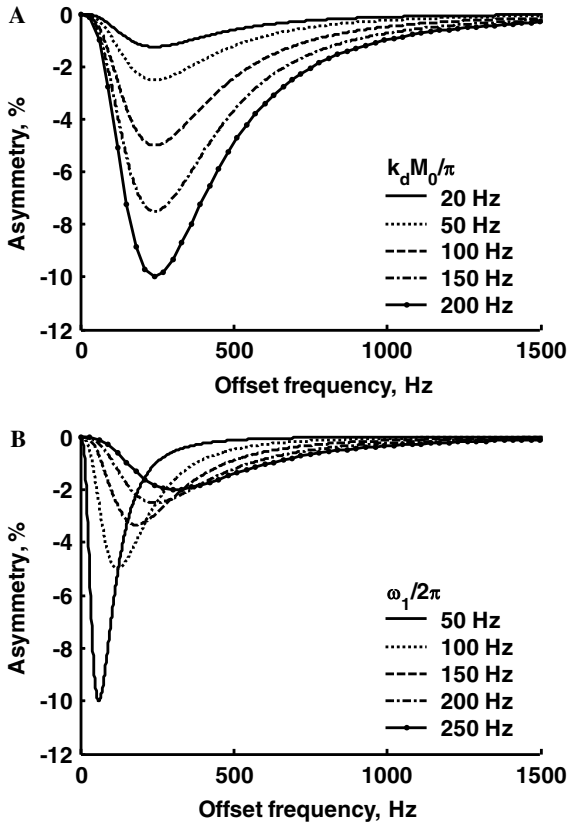

Fig. 2. (A) Simulations of Z-spectrum asymmetry at $\theta = -45°$ for a fixed radiofrequency field amplitude $\omega_1/2\pi$ of 200 Hz and radiation damping fields $k_d M_0/\pi$ of 20–200 Hz; other parameters as for Fig. 1A. (B) $\omega_1/2\pi$ varying from 50–250 Hz, $k_d M_0/\pi$ fixed to 50 Hz; other parameters as Fig. 1A.

Two one-pool Z-spectra acquired at relatively extreme electrical detuning positions, off-resonance by -0.50 MHz and $+1.00$ MHz, are shown in Fig. 3A; the asymmetry due to probe detuning is evident. The accuracy of the solution to the modified Bloch equations was tested by fitting the solution of Eq. (3) to the experimental Z-spectra. Initially the data were fitted with the unsaturated water peak integral (S_0), the exact resonance frequency of water (f_0) and the RD constant ($k_d M_0$) as variable parameters. Unlike S_0, $k_d M_0$ is expected to remain constant with probe detuning, and indeed only moderate, unsystematic variation was observed in the fitting procedure. The value of $k_d M_0$ was fixed to an average from all nine experiments, and a second phase of fitting was run with only S_0 and f_0 as free parameters.

The fitted values of S_0 behave as expected; as the probe is detuned, the probe efficiency decreases and consequently there is less signal. Interestingly, fitting the small flip angle spectra and the Z-spectra yields different estimates of the radiation damping strength, the former giving a value of $k_d M_0/\pi$ of 47 Hz and the latter 35 Hz, 25% lower. As Augustine has pointed out, the effects of RD are complicated significantly by inhomogeneous fields [24]. Numerical simulations using multiple closely spaced isochromats were

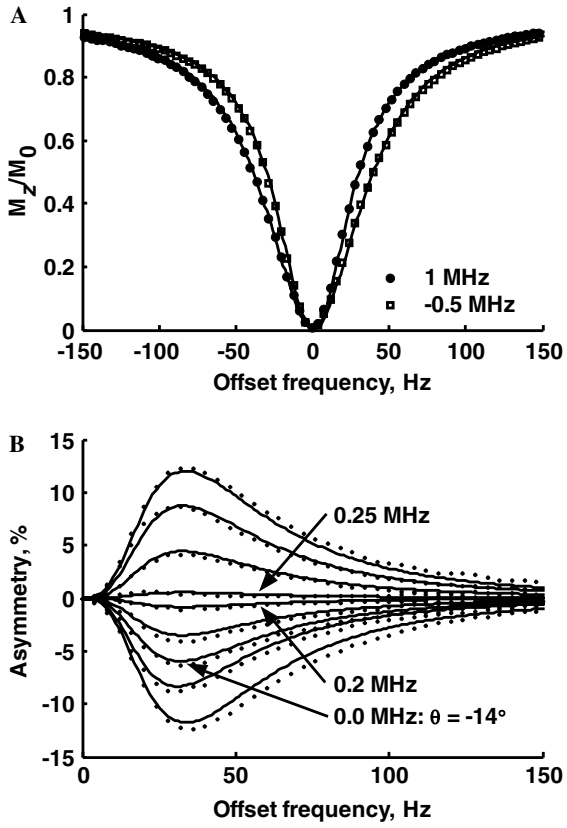

Fig. 3. (A) Experimental Z-spectra acquired for a 90% H_2O / 10% D_2O mixture in a 5 mm NMR tube, with the probe detuned by +1.00 MHz (closed circles) and by −0.50 MHz (open squares). The solid lines represent the results of fitting the solution of Eq. (3) to the data, with f_0 and S_0 as variable parameters. (B) Experimental asymmetry plots calculated from the interpolated Z-spectra and asymmetry curves of the fitted Z-spectra. The tuning offsets, listed from top to bottom, were +1.00, +0.60, +0.40, +0.25, +0.20, +0.10, 0.00, −0.10 and −0.50 MHz. Note that these offsets are from the nominal electrical resonance found by minimizing the reflected RF power, not from true electrical resonance, so at 0.00 MHz θ is nonzero.

performed for the two experiments, and showed that while B_0 inhomogeneity further broadens the resonance line in a simple spectrum, as expected, the effect on the Z-spectrum is to reduce the effect of radiation damping. Experimental Z-spectra thus show a significant reduction in the effective damping strength; the relatively poor B_0 inhomogeneity *in vivo* should therefore help to reduce the impact of RD on Z-spectrum asymmetry.

The relaxation parameters, α (0.31 s^{-1}) and β (0.45 s^{-1}), were fixed at the values determined by inversion recovery and CPMG experiments, respectively. The position of exact electrical resonance and the loaded probe quality factor Q of 210, which was determined by fitting the signal phase to Eq. (5), were used to calculate the detuning angle θ as a function of frequency using Eq. (2). These data also showed that with the spectrometer, sample and probe used, electrical resonance was approximately 0.23 MHz ($\theta = -14°$) from the position of minimum reflected power.

The asymmetry plots for one-pool are shown in Fig. 3B. Comparison between the experimental asymmetry plots and the theoretical curves shows excellent agreement. As expected, the data show a systematic variation in asymmetry as the tuning is varied. Although the asymmetry can exceed 10% of the unsaturated water signal, perhaps the most striking result is at nominal electrical resonance, where the probe is supposed to be perfectly tuned. Here the asymmetry still amounts to around 5% of the total spectrum amplitude, highlighting the sensitivity of the Z-spectrum to probe tuning. For comparison, in *in vivo* experiments, the asymmetry due to chemical exchange between macromolecules and water is typically 1–2% [41].

4.3. Two-pool model

Fig. 4 shows the experimental asymmetry plots, interpolated as described above, for three different tuning positions, compared with the theoretical curves. The measured Z-spectral asymmetry was fitted to the two-pool solutions of Eq. (8) for a solution of urea. As with the one-pool model, the fitting was a two-stage process in which k_d, S_0 and f_0 were the initial variable parameters, and then k_d was fixed at its average value for all datasets. As in the one-pool case, a reduction in apparent k_d is observed. The on-resonance linewidth in a small flip-angle spectrum implied a $k_d M_0/\pi$ of 35 Hz, while fitting the Z-spectra gave 26 Hz. α_a was determined from inversion recovery experiments and fixed at 0.26 s^{-1}. The large excess of **a** (water) magnetization and the relatively rapid exchange (see below) between **a** and **b** pools mean that the spin–lattice relaxation of the system is dominated by the water contribution, so α_b was fixed at the same value. The transverse relaxation rates, β_a and β_b, were fixed at 0.38 s^{-1} and 150 s^{-1}, respectively, the former determined using a CPMG experiment and the latter from the spectral linewidth. The detuning angle θ was determined from Eq. (2). The exchange rate R_b from pool **b** to pool **a** was found by iterative fitting of the results of a Hoffman–Forsén exchange experiment [28] on the same 0.32 M urea sample and fixed at 1.7 s^{-1}.

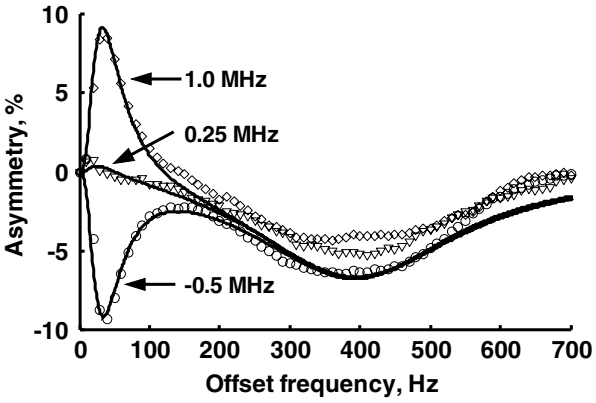

Fig. 4. Experimental asymmetry plots calculated from the interpolated Z-spectra and asymmetry curves of the fitted Z-spectra for pH 7 urea solution. Asymmetry plots for three different offsets from nominal electrical resonance are shown; detuned by +1.00 MHz (diamonds), by +0.25 MHz (triangles) and by −0.50 MHz (circles).

The two-pool data show the same general behaviour as reported for the one-pool system, with the expected addition of a dip around 390 Hz arising from the amine protons of the urea exchanging with the water protons of the buffer solution. Although the difference between experimental data and simulation is slightly greater than for the one-pool system, the effects of electrical detuning, in the presence of RD, on the asymmetry plots are well described by the modified Bloch equations.

It is clear from Fig. 4 that here the effects due to RD can easily exceed the Z-spectral asymmetry due to exchange of protons, even though the concentration of the urea is an order of magnitude larger than the concentration of exchangeable protons expected *in vivo*. In these experiments the peak of the exchange asymmetry, at the chemical shift of the urea NH protons, is much closer (390 Hz) to the water resonance than is the case *in vivo*, suggesting that *in vivo* there might be relatively little crosstalk between the sources of asymmetry. Unfortunately, the displacement of the RD asymmetry peak maximum from the water resonance is proportional to ω_1 (see Fig. 2B), so at the higher saturating RF powers recommended for *in vivo* experiments [46] there may still be some difficulty disentangling the effects of RD and exchange.

While the radiation damping rates discussed so far are typical of medium-field high-resolution spectrometers, most Z-spectroscopy is carried out on imaging instruments. Here the damping rate will be considerably smaller because the static magnetic field, coil quality factor (Q) and filling factor are all usually lower. To investigate the potential effect of RD in such systems, a simulation was run with a damping field $k_d M_0/\pi$ of 8 Hz, corresponding to a 200 MHz instrument with a filling factor of 0.25 and a Q of 100. Other parameters were set as follows: $\omega_1/2\pi = 110$ Hz (as recommended by Sun et al. [46]), an exchange rate constant $R_b = 30\ s^{-1}$, chemical shift difference between exchanging species and water 3.5 ppm, equilibrium constant $R_b/R_a = 1250$, relaxation parameters $\alpha_a = 0.50\ s^{-1}$, $\alpha_b = 0.50\ s^{-1}$, $\beta_a = 10\ s^{-1}$ and $\beta_b = 200\ s^{-1}$. With these parameters the Z-spectra and exchange effects are similar to those measured *in vivo* at 200 MHz from rat brain [41]. Simulated Z-spectrum asymmetry curves for probe phase angles θ of +45°, −45°, +4.5° and −4.5° are presented in Fig. 5. The amplitude of radiation damping-induced asymmetry is relatively small, but the peak is broad enough to disturb both the shape and the amplitude of the exchange-induced main peak.

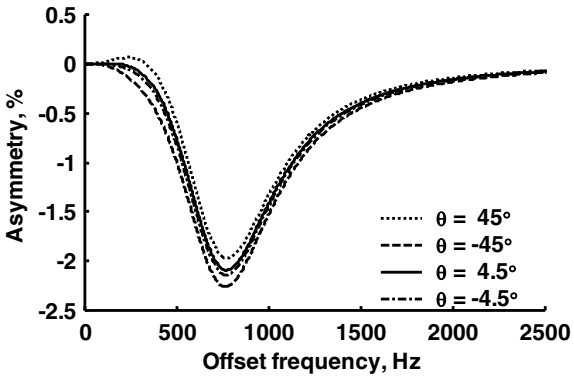

Fig. 5. Simulated asymmetry curves for a two-pool exchanging system corresponding to a typical *in vivo* experiment at 200 MHz. A filling factor of 0.25, Q of 100, exchange rate R_b of 30 s^{-1}, equilibrium constant of 1250, 3.5 ppm chemical shift difference between the two magnetization pools, radiofrequency field amplitude $\omega_1/2\pi$ of 110 Hz and a radiation damping field $k_d M_0/\pi$ of 8 Hz were used. The relaxation parameters were $\alpha_a = 0.50\ s^{-1}$, $\alpha_b = 0.50\ s^{-1}$, $\beta_a = 10\ s^{-1}$ and $\beta_b = 200\ s^{-1}$. Traces are shown for a damped system with four different offsets from electrical resonance.

4.4. RD in experiments with short saturation time

In many *in vivo* imaging experiments it is not practicable to irradiate the water pool for a sufficient time to achieve a true steady state, either because of prohibitively long scan times or because of SAR limits. The effect of RD on experiments with shorter irradiation times was therefore studied experimentally. Two samples of a 90% H_2O/10% D_2O mixture were used, one in a standard 5 mm NMR tube, giving an RD field $k_d M_0/\pi$ of 47 Hz, and one in a 2 mm outside diameter tube, giving a damping field of 6 Hz. Sample size restriction was used in preference to dilution in order to keep the sample relaxation properties the same; a sample diluted down to 1% H_2O/99% D_2O in a 5 mm tube showed negligible RD effects.

Experimental Z-spectra measured at exact electrical resonance using a pre-irradiation time of 2 s, rather than the 20 s used previously, are shown in Fig. 6A. The comparison between the two samples shows that while the Z-spectrum has the usual form, RD has a much more marked effect than at steady state (compare the nearly identical undamped and damped ($\theta = 0$) traces in Fig. 1A). This is because the amount of transverse magnetization, and hence the secondary RF field induced, is much greater than at steady state. At this shorter irradiation time the effects of RD are more florid; Fig. 6B–D show the measured M_z as a function of saturation time for the 2 mm tube, M_z for the 5 mm tube, and the difference between the two, respectively. Radiation damping dramatically changes the early course of the approach to steady state in these experiments. In practical experiments *in vivo*, the much poorer field homogeneity is likely to damp the transverse magnetization earlier in the saturation, but problems are still likely with short saturation times.

5. Conclusions

The effects of radiation damping and probe detuning on the shape and asymmetry of Z-spectra have been explored. For concentrated samples at high field, radiation damping significantly narrows the Z-spectrum. The narrowing occurs because the secondary RF field induced by the rotating transverse magnetization opposes the effects of the applied B_1 field. When the radiation damping takes

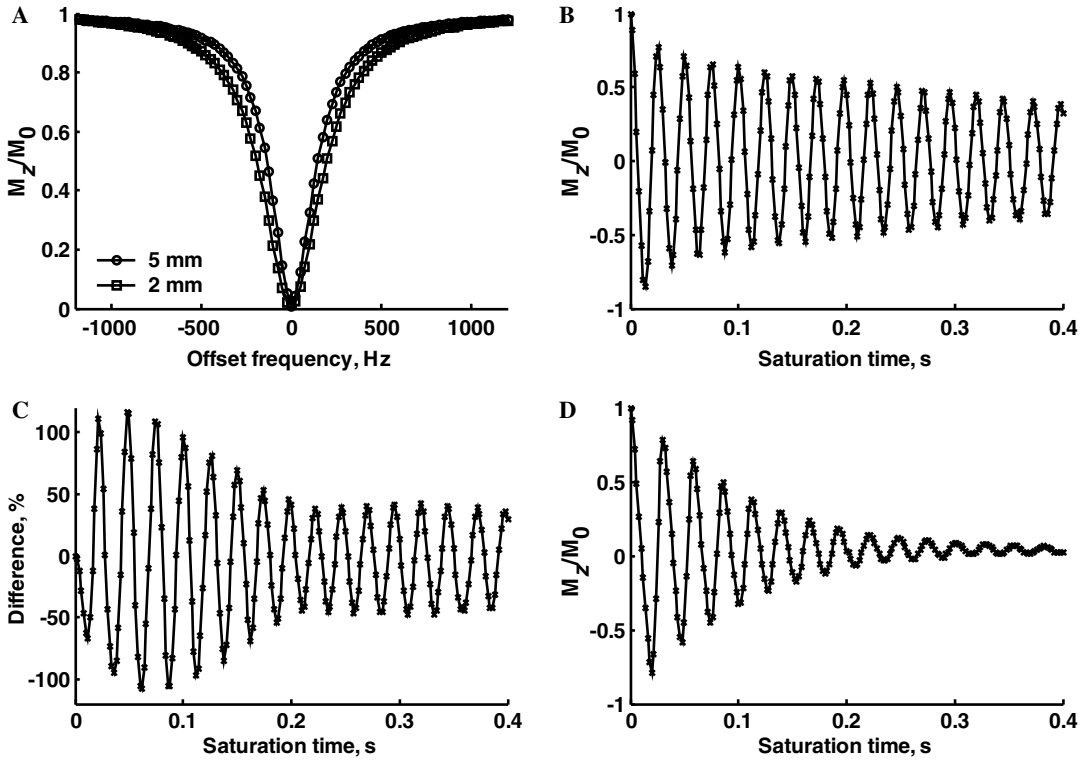

Fig. 6. (A) Experimental Z-spectra measured with a 2 s saturation pulse for a 90% H_2O/10% D_2O sample in a 5 mm o.d. NMR tube (circles) and in a 2 mm o.d. tube (squares). The RD constants $k_d M_0/\pi$ were 47 Hz and 6 Hz, respectively. (B) Water Z-magnetization as a function of pre-irradiation time for the 5 mm sample; (C) for the 2 mm sample; and (D) difference between (A) and (C).

place in an imperfectly tuned probe, an asymmetry is also introduced into the Z-spectrum. Even a slight deviation from electrical resonance, common when using conventional tuning methods, is enough to produce RD-induced asymmetry comparable in magnitude to the asymmetry due to chemical exchange. This could in some cases obscure the pH-dependent information in Z-spectra. Increasing the amplitude of the saturation pulse can reduce the relative effect of the RD damping, but this shifts the position of maximum asymmetry due to RD further away from the water resonance. For the lower and less homogeneous magnetic fields generally used for *in vivo* experiments, the RD effects will be considerably smaller than those measured here; however the simulations presented suggest that under some circumstances they could still exert a significant influence on the asymmetry of the Z-spectrum. In studies *in vivo*, especially in a clinical environment, it is often necessary to limit examination time, and long saturation pulses are generally undesirable. In such experiments, the results reported here show that the effects of radiation damping can be much larger than where a true steady state is reached.

Acknowledgments

Financial support from the Sigrid Juselius Foundation (JN), the Academy of Finland (JN) and the Leverhulme Trust (grant F00120Y to GAM and RAK) is greatly appreciated.

References

[1] X.A. Mao, J.X. Guo, C.H. Ye, Chem. Phys. Lett. 227 (1994) 65–68.
[2] X.A. Mao, J.X. Guo, C.H. Ye, Chem. Phys. Lett. 222 (1994) 417–421.
[3] J.H. Chen, X.A. Mao, C.H. Ye, J. Magn. Reson. A 123 (1996) 126–130.
[4] J. Grad, R.G. Bryant, J. Magn. Reson. 90 (1990) 1–8.
[5] M.H. Levitt, Concepts Magn. Reson. 8 (1996) 77–103.
[6] G. Suryan, Curr. Sci. 18 (1949) 203–204.
[7] N. Bloembergen, R.V. Pound, Phys. Rev. 95 (1954) 8–12.
[8] C.R. Bruce, R.E. Norberg, G.E. Pake, Phys. Rev. 104 (1956) 419–420.
[9] S. Bloom, J. Appl. Phys. 28 (1957) 800–805.
[10] A. Szöke, S. Meiboom, Phys. Rev. 113 (1959) 585–586.
[11] W.S. Warren, J. Chem. Phys. 91 (1989) 5895–5904.
[12] H. Barjat, G.P. Chadwick, G.A. Morris, A.G. Swanson, J. Magn. Reson. A 117 (1995) 109–112.
[13] M. Guéron, P. Plateau, M. Decorps, Prog. Nucl. Magn. Reson. Spectrosc. 23 (1991) 135–209.
[14] J.H. Chen, X.A. Mao, J. Chem. Phys. 107 (1997) 7120–7126.
[15] J.H. Chen, X.A. Mao, J. Magn. Reson. 131 (1998) 358–361.
[16] G.E. Ball, G.J. Bowden, T.H. Heseltine, M.J. Prandolini, W. Bermel, Chem. Phys. Lett. 261 (1996) 421–424.
[17] A. Vlassenbroek, J. Jeener, P. Broekaert, J. Chem. Phys. 103 (1995) 5886–5897.
[18] J. Zhou, S. Mori, P.C. van Zijl, Magn. Reson. Med. 40 (1998) 712–719.
[19] K. Teh, N. de Zanche, J. Wild. in Proceedings of the ISMRM 14th Scientific Meeting & Exhibition, vol. 1, pp. 218, Seattle, WA, 2006.
[20] X.A. Mao, D.H. Wu, C.H. Ye, Chem. Phys. Lett. 204 (1993) 123–127.
[21] X.A. Mao, J.X. Guo, C.H. Ye, Chem. Phys. Lett. 218 (1994) 249–253.
[22] J.X. Guo, X.A. Mao, Phys. Rev. B: Condens. Matter 50 (1994) 13461–13466.
[23] C. Szantay, A. Demeter, Concepts Magn. Reson. 11 (1999) 121–145.
[24] M.P. Augustine, E.L. Hahn, Concepts Magn. Reson. 13 (2001) 1–7.

[25] M.P. Augustine, Prog. Nucl. Magn. Reson. Spectrosc. 40 (2002) 111–150.
[26] X.A. Mao, C.H. Ye, Concepts Magn. Reson. 9 (1997) 173–187.
[27] S.Y. Huang, C. Anklin, J.D. Walls, Y.Y. Lin, J. Am. Chem. Soc. 126 (2004) 15936–15937.
[28] S. Forsén, R.A. Hoffman, J. Chem. Phys. 39 (1963) 2892–2901.
[29] J. Grad, D. Mendelson, F. Hyder, R.G. Bryant, J. Magn. Reson. 86 (1990) 416–419.
[30] S.D. Wolff, R.S. Balaban, Magn. Reson. Med. 10 (1989) 135–144.
[31] X.Z. Wu, J. Magn. Reson. 94 (1991) 186–190.
[32] G.H. Caines, T. Schleich, J.M. Rydzewski, J. Magn. Reson. 95 (1991) 558–566.
[33] R.M. Henkelman, X.M. Huang, Q.S. Xiang, G.J. Stanisz, S.D. Swanson, M.J. Bronskill, Magn. Reson. Med. 29 (1993) 759–766.
[34] K. Kuwata, D. Brooks, H. Yang, T. Schleich, J. Magn. Reson. B 104 (1994) 11–25.
[35] C. Morrison, G. Stanisz, R.M. Henkelman, J. Magn. Reson. B 108 (1995) 103–113.
[36] H.I. Mäkela, O.H. Gröhn, M.I. Kettunen, R.A. Kauppinen, Biochem. Biophys. Res. Commun. 289 (2001) 813–818.
[37] G.J. Stanisz, A. Kecojevic, M.J. Bronskill, R.M. Henkelman, Magn. Reson. Med. 42 (1999) 1128–1136.
[38] T. Ceckler, J. Maneval, B. Melkowits, J. Magn. Reson. 151 (2001) 9–27.
[39] J.Y. Zhou, J.F. Payen, P.C.M. van Zijl, Magn. Reson. Med. 53 (2005) 356–366.
[40] K.M. Ward, R.S. Balaban, Magn. Reson. Med. 44 (2000) 799–802.
[41] J. Zhou, J.F. Payen, D.A. Wilson, R.J. Traystman, P.C.M. van Zijl, Nat. Med. 9 (2003) 1085–1090.
[42] J. Zhou, D.A. Wilson, P.Z. Sun, J.A. Klaus, P.C.M. van Zijl, Magn. Reson. Med. 51 (2004) 945–952.
[43] F. Bloch, Phys. Rev. 70 (1946) 460–474.
[44] J.W.S. Harris, Handbook of Mathematics and Computational Science, Springer-Verlag, New York, Berlin, Heidelberg, 1998.
[45] W.H. Press, S. Teukolsky, W.T. Vetterling, B.P. Flannery, Numerical Recipies in C, second ed., Cambridge University Press, Cambridge, 1994.
[46] P.Z. Sun, P.C.M. van Zijl, J. Zhou, J. Magn. Reson. 175 (2005) 193–200.